

# Pigment Epithelium-Derived Factor (PEDF) Binds to Glycosaminoglycans: Analysis of the Binding Site

Elena Alberdi, C. Craig Hyde,<sup>‡</sup> and S. Patricia Becerra\*

Laboratory of Retinal Cell and Molecular Biology, NEI, NIH, Building 6, Room 308, 6 Center Drive MSC 2740, Bethesda, Maryland 20892-2740

Received January 29, 1998; Revised Manuscript Received May 21, 1998

**ABSTRACT:** Pigment epithelium-derived factor (PEDF), a neurotrophic protein, is a secreted serpin identified in extracellular matrixes. We show that PEDF extractions from the interphotoreceptor matrix are more efficient with increasing NaCl concentrations, indicating that ionic interactions mediate its association with this polyanionic matrix. We have used affinity chromatography and ultrafiltration to probe for direct binding of PEDF to glycosaminoglycans/polyanions. Correctly folded PEDF bound to immobilized heparin, chondroitin sulfate-A, -B, -C, and dextran sulfate columns and eluted from each with an increase in NaCl concentration. However, in the presence of urea, the protein lost its affinity for heparin. Binding of PEDF to heparan sulfate proteoglycan in solution was in a concentration-dependent fashion (half-maximal specific binding  $EC_{50} = 40 \mu\text{g/mL}$ ) and was sensitive to increasing NaCl concentrations. The glycosaminoglycan-binding region was analyzed using chemical modification and limited proteolysis. PEDF chemically modified on lysine residues by biotinylation lost its capacity for interacting with heparin, implicating the involvement of PEDF lysine residues in heparin binding. Cleavage of the serpin-exposed loop with chymotrypsin did not affect the heparin-binding property. A limited proteolysis product containing residues 21–~260 bound to heparin with similar affinity as the intact PEDF. Homology modeling of PEDF based on the X-ray crystal structures of antithrombin III and ovalbumin shows a region at the center of  $\beta$ -sheet A—strands 2 and 3—and helix F that has a basic electrostatic surface potential and is densely populated with lysines exposed to the surface (K134, K137, K189, K191, H212, and K214) that are available to interact with various glycosaminoglycans/polyanions. This region represents a novel site for glycosaminoglycan binding in a serpin, which in PEDF, is distinct and nonoverlapping from the PEDF neurotrophic active region.

Glycosaminoglycans and proteoglycans are found predominantly in association with cell surfaces as structural components and functional modulators of extracellular matrixes (1). Glycosaminoglycans are highly sulfated and negatively charged polymers of disaccharide repeats, and proteoglycans are complex glycoconjugates containing a core protein to which several glycosaminoglycan chains (such as heparin, heparan sulfate, chondroitin sulfate, etc.) are covalently attached (2). Cell-surface-associated glycosaminoglycans are thought to act in combination with extracellular proteins as regulators of the neuronal pattern formation, survival, and function. They are required for the interaction of several growth/trophic factors with cell surface receptors and are binding components for cell adhesion proteins (12–17). Structurally diverse glycosaminoglycans and proteoglycans are abundant in the developing and mature CNS (3–5). Heparan and chondroitin sulfate-containing proteoglycans are spatially and temporally distributed across the extracellular spaces of the developing neural retina (3, 6–8). In the mature retina, these macromolecules maintain a spatial distribution, which is found altered under pathological

conditions, e.g., photoreceptor degeneration, age-related maculopathy, diabetes (4, 9–11).

Pigment epithelium-derived factor (PEDF)<sup>1</sup> is a 50 kDa secreted glycoprotein identified in the eye in the interphotoreceptor matrix—the extracellular matrix between the retinal pigment epithelium and the neural retina and vitreous and aqueous humor (18–20). It is also identified in cultured media of a variety of cells, such as cultured retinal pigment epithelial, ciliary epithelial, fibroblast cells, and cell-lines harboring PEDF cDNA expression vectors (20–23). PEDF has several neurotrophic properties *in vitro* that support a role for PEDF in neuronal cell differentiation and survival and cell maintenance. Addition of nanomolar concentrations of the protein induces neuronal differentiation in cultured retinoblastoma cells (21, 24) and protects primary cultures of cerebellar neurons against natural cell death (25) and glutamate neurotoxicity (26). In addition, in the fibroblast WI-38 cell line, expression of the PEDF gene is >100-fold

\* Corresponding author. Phone: 301-496-6514. Fax: 301-402-9211. E-mail: pbecerra@helix.nih.gov.

<sup>‡</sup> Laboratory of Structural Biology Research, NIAMS, NIH, Bethesda, MD 20892.

<sup>1</sup> Abbreviations: PEDF, pigment epithelium-derived factor; serpin, serine protease inhibitor; rhPEDF, recombinant human PEDF; Ab-rPEDF, polyclonal antiserum to PEDF; HSPG, heparan sulfate proteoglycan; MWCO, molecular weight cutoff; PBS, phosphate buffered saline; sulfo-NHS-LC-biotin, sulfo-*N*-hydroxysuccinimide-LC-Biotin; HABA, 2-(4'-hydroxyazobenzene) benzoic acid; PDB, Protein Data Bank.

<sup>2</sup> Alberdi, E., and Becerra, S. P. Personal observations.

higher in young cells than in their senescent counterparts (22).

The sequence of the PEDF cDNA reveals that PEDF is a member of the serpin (serine protease inhibitor) superfamily (21, 22). Although the protein has the overall protein conformation of a serpin, it does not have a demonstrable inhibitory activity against proteases, and behaves like the noninhibitory serpins ovalbumin, angiotensinogen, and maspin (27). A neurotrophic active region is separated from the homologous protease-binding site, the serpin-exposed loop, in the PEDF sequence, indicating that the PEDF neurotrophic activity is not mediated by inhibition of proteases. Given that PEDF coexists with glycosaminoglycans/proteoglycans in extracellular matrixes and has neurotrophic properties, it is of interest to study the interactions between this serpin protein and these polysaccharides at a molecular level.

In a previous study, we have shown that purified human recombinant PEDF interacts with a heparin molecule composed of 30 sugars (23). Here, we show that PEDF is naturally associated with the bovine interphotoreceptor matrix by ionic interactions, and the characterization of its binding to several glycosaminoglycans/polyanions, including heparan and chondroitin sulfates, using purified native bovine and recombinant human protein. We have used chemical modification, limited proteolysis and a predictive spatial model to analyze a glycosaminoglycan-binding region on the PEDF amino acid sequence. Contributions of positively charged regions for glycosaminoglycan binding in a spatial model of PEDF are discussed.

## EXPERIMENTAL PROCEDURES

**Materials.** Heparin acrylic beads (0.7 mg of heparin/mL), heparan sulfate proteoglycan (HSPG), bovine trachea chondroitin sulfate A, bovine mucosa chondroitin sulfate B (dermatan sulfate), shark cartilage chondroitin sulfate C, Epoxy Sepharose 6B, and sulfated dextran beads were purchased from Sigma. Human plasma heparin cofactor II was obtained from Calbiochem; ovalbumin from Pharmacia; EZ-Link sulfo-*N*-hydroxysuccinimide-LC-biotinylation kit and SuperSignal CL-HRP substrate system were purchased from Pierce Chemical Co.;  $\alpha$ -chymotrypsin was from Worthington, Inc.

**Extraction of Proteins from Interphotoreceptor Matrix.** Adult bovine eyes were obtained from J. W. Trueth and Sons (Baltimore, MD). All procedures were performed at 4 °C. The soluble components of the interphotoreceptor matrix were obtained as described previously (18), except for the following extraction solutions: 20 mM NaCl, 150 mM NaCl, or 1.5 M NaCl in a buffer containing 20 mM sodium phosphate buffer, pH 6.5, and 10% glycerol.

**Preparation of PEDF.** Native PEDF protein was purified from the interphotoreceptor matrix and vitreous of fresh bovine eyes, as described previously (18, 19). Recombinant PEDF was produced using baby hamster kidney (BHK) cells containing the expression vector pMA-PEDF with a full-length human PEDF cDNA and the protein was purified from the conditioned medium (23).

**Immunoblot Analysis.** Western transfers, immunoreactions, and immunostaining with 4-chloro-naphthol were performed as described previously (18). Enhanced chemiluminescence was performed with SuperSignal (Pierce) following manufacturer's protocol and after immunoreaction

with Ab-rPEDF diluted 1:10000, followed with peroxidase labeled goat antirabbit IgG (H + L) antibody (Kirkegaard & Perry Laboratories, Inc.) diluted 1:15000 using a suspension of 10% nonfat dry milk in 1% normal goat serum, 20 mM Tris-Cl, 150 mM NaCl, and 0.05% Tween-20. Quantification of immunoreactive PEDF proteins was performed by densitometric scanning using a GSXL software program (Pharmacia).

**Preparation of Chondroitin Sulfate-Sepharose 6B.** A total of 2 g of epoxy-activated Sepharose 6B was swollen and washed on a sintered glass filter with distilled water. Two milliliters of swollen gel were added to 2 mL of coupling solution, containing 0.1 M boric acid, pH 10, and 80 mg each of chondroitin sulfate A, chondroitin sulfate B, or chondroitin sulfate C. Each coupling reaction was performed by mixing in an incubator shaker at 37 °C for 16 h. The excess ligand was washed successively with 150 mL of 0.1 M boric acid, pH 10; 100 mL of deionized water; 100 mL of 0.1 M sodium bicarbonate, pH 8; and, finally, 100 mL of 0.1 M sodium acetate, pH 4. The remaining active groups in each coupled gel were blocked with one column volume of 1 M ethanolamine mixing at 37 °C for 16 h using an incubator shaker. Each coupled Sepharose 6B was then washed successively with 100 mL of 0.1 M boric acid, pH 10; 100 mL of 0.1 M sodium acetate/0.5 M sodium chloride, pH 4; and, finally, 100 mL of 0.1 M boric acid/0.5 M sodium chloride, pH 8.

**Glycosaminoglycan-Affinity Column Chromatography.** Affinity resins were packed in Polyprep chromatography columns (Bio-Rad) to yield 0.5 mL settled bed volume and equilibrated with buffer H (20 mM NaCl, 20 mM sodium phosphate, pH 6.5 and 10% glycerol). A solution of purified protein in buffer H was applied to the appropriate affinity column and incubated with the resin at 4 °C for 30 min. The glycosaminoglycan-affinity columns were washed with more than 10 column volumes of the incubation buffer and eluted with a NaCl step-gradient in buffer H at 1.5 column volumes per fraction and as indicated. Aliquots from each fraction were analyzed by SDS-PAGE.

**Radiolabeled [<sup>125</sup>I]PEDF.** Bovine PEDF protein was radiolabeled with <sup>125</sup>I using an immobilized form of *N*-chlorobenzenesulfonamide (sodium salt), the Iodo-beads Iodination Reagent (Pierce Chemical, Co.), as prepared by Lofstrand Laboratories. The radiolabeled protein was separated from the precursor by Sephadex G25 column chromatography in PBS containing 0.15% gelatin. The specific activity of the final sample was determined after immunoblotting using Ab-rPEDF (18) to quantify the amount of PEDF protein and radioactivity measurement from the excised immunostained PEDF band using a liquid scintillation  $\beta$ -counter (Beckman, model LS 3801).

**HSPG-PEDF Binding Assays.** Bovine PEDF at 120  $\mu$ g/mL or ovalbumin at 100  $\mu$ g/mL was each mixed with HSPG in buffer H in a final volume of 100  $\mu$ L. The mixtures were incubated at 4 °C for 30 min and then ultrafiltered through Centricon-100 (Amicon). The concentrated material was diluted 20-fold with incubation buffer and ultrafiltered four times. The filtered protein was concentrated using a Centricon-30 device. Aliquots of the concentrated samples were analyzed by SDS-PAGE.

Radiolabeled [<sup>125</sup>I]PEDF at 91.5 ng/mL (6.25  $\mu$ Ci/mL) and increasing concentrations of HSPG were mixed in buffer H

(10  $\mu$ L) and incubated at 4 °C for 30 min. Free and bound PEDF was separated by ultrafiltration through Microcon-100 (Amicon). The concentrated material was diluted 40-fold with incubation buffer and washed as described above. Each Microcon retentate cup was transferred to a scintillation vial and mixed with 5 mL of Bio-Safe II liquid scintillation solution (Research Products International, Corp.) by extensive vortexing. Radioactivity was determined using a  $\beta$ -counter (Beckman, model LS 3801).

**Biotinylation of PEDF.** Biotin was coupled onto PEDF with sulfo-*N*-hydroxysuccinimide-LC-biotin following the manufacturer's protocol. Briefly, to a solution of PEDF at 2 mg/mL in phosphate buffered saline (PBS = 20 mM sodium-phosphate, 150 mM NaCl) was added sulfo-NHS-LC-biotin to a final concentration of 0.5 mg/mL and left to react at room temperature for 30 min. The reaction mixture was ultrafiltered and washed three times with ice-cold PBS, using Centricon-30 (Amicon) devices, to remove any free biotinylation reagent. Biotin incorporation was determined by the HABA [2-(4'-hydroxyazobenzene)benzoic acid] (Pierce) method (28) following the manufacturer's recommendations. Biotinylated PEDF (final concentration 70 ng/ $\mu$ L) was added to a mixture of HABA at 0.28 mM and an excess of avidin (0.46 mg/mL) in phosphate buffered saline. The concentration of incorporated biotin was calculated from the difference in absorbance at 500 nm ( $A_{500\text{ nm}}$ ) between mixture without and with biotinylated protein ( $\Delta A_{500} = A_{500, \text{ of HABA reagent}} - A_{500, \text{ biotinylated-PEDF}}$ ) and the  $\Delta \epsilon_{500}$  (=34 000), the apparent  $\Delta \epsilon$  calculated from the change in optical density following addition of excess biotin when the concentration of HABA-avidin is 0.25 mM, equal to  $\Delta A_{500}/\text{mol of biotin bound/L}$ . The degree of biotinylation was calculated using the ratio of the biotin concentration in micromoles per milliliter of sample and the PEDF protein concentration. These conditions resulted in a biotin-modified PEDF with 4.2 biotins/molecule of protein. Detection of biotinylated PEDF was performed on a western transfer (nitrocellulose membrane) using avidin-biotinylated horseradish peroxidase complex (Vectastain ABC kit, Vector laboratories), followed by the development of a light-producing reaction by enhanced chemiluminescent system using SuperSignal CL-HRP substrate System.

**Preparation of Cleaved PEDF.** PEDF was treated with  $\alpha$ -chymotrypsin using a substrate:protease ratio of 100:1 (w/w) for 60 min at 25 °C, yielding a 46 kDa PEDF proteolytic fragment (27). A chymotryptic 30 kDa polypeptide fragment was obtained using a ratio of 1:1 (w/w) for 15 min at 25 °C. The chymotrypsin reaction mixtures were in 20 mM Tris/HCl, pH 7.5, 150 mM NaCl, and 1 mM EDTA. PEDF cleavage was confirmed by SDS-PAGE analysis and the N-terminal sequence determination of the polypeptide products.

**Homology Modeling of PEDF.** Three-dimensional homology models of human PEDF were constructed on a Silicon Graphics computer graphics workstation using the LOOK software (version 2.0, Molecular Applications Group) using the SegMod approach, structure database, automatic sequence alignment, and the full refinement options. The amino acid sequence of PEDF was obtained from Swiss-Prot database (29) under accession number P36955. Numbering of PEDF residues is relative to the precursor form, and residues 21–418 comprising the mature protein were used for modeling.

Two models, PEDF<sub>OVA</sub> and PEDF<sub>ATIII</sub>, were constructed based on different serpin structures: ovalbumin (a noninhibitory, nonheparin-binding serpin) and the uncleaved form of antithrombin III (an inhibitory, heparin-binding serpin). PEDF<sub>OVA</sub> was based on the crystal structure of the "A" chain of ovalbumin (30), one of four chains in the crystallographic asymmetric unit [Protein Data Bank (31, 32) designation 1OVA]. PEDF<sub>ATIII</sub> was built using coordinates for the "I" chain of antithrombin III (33) (PDB designation 2ANT). The side-chain rotamers of lysine and arginine residue side-chain atoms were changed (program CHAIN, Version 7.2, Baylor University) to match more closely the conformations observed in the crystal structures. The N-terminal sequence of mature PEDF (positions 21–51) was modeled only based on the antithrombin III structure, since the ovalbumin sequence starts its alignment with the PEDF residue position 52 at the N-terminus of helix A. The two resulting models of PEDF, PEDF<sub>OVA</sub> and PEDF<sub>ATIII</sub>, agree with each other, except in the region of the serpin-exposed loop. Following least-squares superposition of the two PEDF models, more than 90% of the  $\alpha$ -carbon atoms paired within about 4 Å and showed a root-mean-square difference in position of 1.6 Å. Surface electrostatic properties were visualized with the program GRASP (Version 1.2, A. Nicholls, Columbia University) and the averaged potential of PEDF<sub>OVA</sub> and PEDF<sub>ATIII</sub> analyzed.

**Other Assays.** Amino acid sequencing was performed using an Applied Biosystems model 477 sequencer following the manufacturer's protocol. Sequence determination of PEDF proteolytic fragments was performed on protein after resolution by SDS-PAGE, followed by transfer to Immobilon poly-(vinylidene difluoride) membrane (Millipore) and staining briefly with Coomassie Blue (27). The membrane pieces containing stained bands were subjected to amino acid sequencing.

## RESULTS

**PEDF Is Associated with Extracellular Matrix by Ionic Interactions.** We have previously identified PEDF in the interphotoreceptor matrix of bovine eyes (18), which is known to contain glycosaminoglycans and proteoglycans that confer a polyanionic nature to this matrix (4, 5). To determine the nature of its association with this matrix, we extracted proteins from bovine interphotoreceptor matrixes with saline solutions of increasing ionic strengths and then determined the relative amount of PEDF. Figure 1 shows that while the total protein content was similar, PEDF protein in the extracts increased with an increase in NaCl concentration from 0.02 to 0.15 to 1.5 M NaCl. The relative amount of PEDF in extracts with NaCl concentrations between 0.15 and 0.5 M NaCl remained constant (data not shown). These results show that the association of PEDF with the interphotoreceptor matrix is mediated by ionic interactions.

**Glycosaminoglycan-Binding Properties of PEDF.** The apparent binding affinity of PEDF for immobilized heparin, chondroitin sulfate-A, -B, and -C was examined by affinity column chromatography using a NaCl step-gradient. Figure 2 shows SDS-PAGE analyses of the eluted fractions from each column. Native PEDF bound to all four glycosaminoglycans (panels A, D, E, and F) and started to elute with 100 mM NaCl. PEDF eluted from heparin and chondroitin



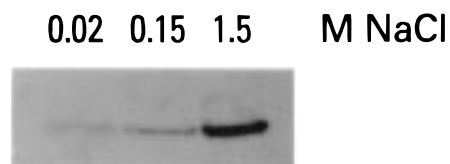


**FIGURE 1:** PEDF immunoreactivity in saline washes of bovine interphotoreceptor matrix. Proteins from the interphotoreceptor matrix of adult bovine eyes were extracted with NaCl-containing solutions using 0.5 mL/eye, concentrations indicated at the top of each lane. A pool of extracts from three eyes was analyzed for PEDF detection. The presence of PEDF in extracts was analyzed by immunoblot analysis with antiserum Ab-rPEDF after SDS–10–20% PAGE. After signal detection with enhanced chemiluminescence, the intensity of the PEDF immunostaining was quantified by densitometry. Samples were applied in a total volume of 18  $\mu$ L containing protein as follows: 0.02 M, 34.7  $\mu$ g; 0.15 M, 36.0  $\mu$ g; 1.5 M, 31.0  $\mu$ g. The relative ratio of intensity for PEDF immunoreactivity is 1 $\times$ , 2 $\times$  and 10 $\times$  for 0.02, 0.15, and 1.5 M NaCl, respectively (averaged from three determinations).

sulfate-C columns with a peak at 150 mM NaCl and from chondroitin sulfate-A and -B columns at 100 mM NaCl. In the presence of 4 M urea, PEDF was detected in the flow-through and wash of the heparin column (Figure 2B). Ovalbumin is a nonheparin-binding serpin and was used as control (Figure 2C). Heparin cofactor II is a serpin found in mammalian plasma that inhibits thrombin >1000 times more rapidly in the presence than in the absence of

chondroitin sulfate B (34). We have compared the affinity of heparin cofactor II for chondroitin sulfate-B to that of PEDF. As shown in Figure 2G, heparin cofactor II bound to chondroitin sulfate-B and started eluting with 50 mM NaCl and a peak at 150 mM NaCl, comparable to that for PEDF. These results show that native PEDF binds to immobilized glycosaminoglycans by ionic interactions and with similar affinities among them; however, unfolded protein is deficient in binding heparin.

**PEDF Binds to HSPG in a Concentration–Response Fashion.** To study the glycosaminoglycan–PEDF interactions in solution, we performed binding assays between native PEDF and HSPG followed by ultrafiltration using anisotropic membranes. This assay is based on the fact that PEDF is a monomeric protein (50 kDa) that filters through a membrane with pores of larger size, e.g., 100 000 MW exclusion limit (see Figure 3A, lane 1). HSPG was chosen since it is a heparan sulfate containing molecule with an apparent molecular mass (>300 kDa) that differs from PEDF by more than 6-fold. Binding of PEDF to HSPG was assayed by separation of bound and unbound PEDF using membranes of 100 000 MWCO, followed by SDS–PAGE analysis of the recovered retained solutes. Figure 3A shows that PEDF was retained only in the presence of HSPG. Quantitation of PEDF protein from stained gels showed that the amount of PEDF retained with 50  $\mu$ g/mL HSPG (lane

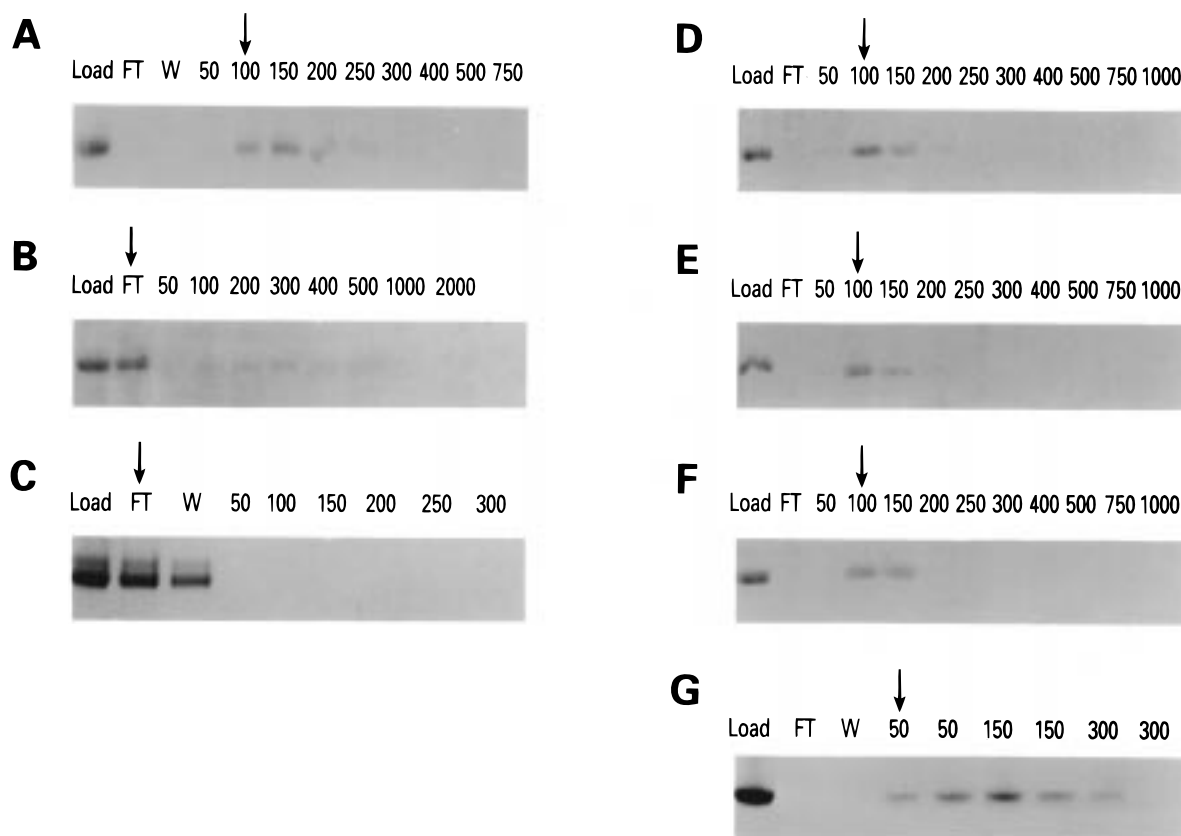


**FIGURE 2:** PEDF binding to glycosaminoglycans. Bovine PEDF was analyzed by affinity column chromatography using heparin acrylic beads (panels A and B) and chondroitin sulfate A-, chondroitin sulfate B-, and chondroitin sulfate C-Sepharose (panels D–F, respectively). In panel B, the PEDF protein sample and chromatography were in the presence of 4 M urea. Ovalbumin was analyzed with heparin acrylic beads (panel C) and heparin cofactor II with chondroitin sulfate-Sepharose as points of comparison (panel G). Each protein sample (30–60  $\mu$ g/mL) was mixed with resin in buffer H at a 1:1 volume ratio and incubated at 4  $^{\circ}$ C for 30 min. The unbound protein was collected in the flow-through (FT) and wash (W) with 10 column volumes of buffer H. The bound proteins eluted with a NaCl step-gradient at 1.5 column volume/fraction (numbers at top of each lane correspond to NaCl concentration in millimolarity). An aliquot from each fraction was resolved by 12.5% SDS–PAGE. Photographs of Coomassie Brilliant blue stained gels are shown. The arrow indicates the fraction at which protein starts eluting from each column.

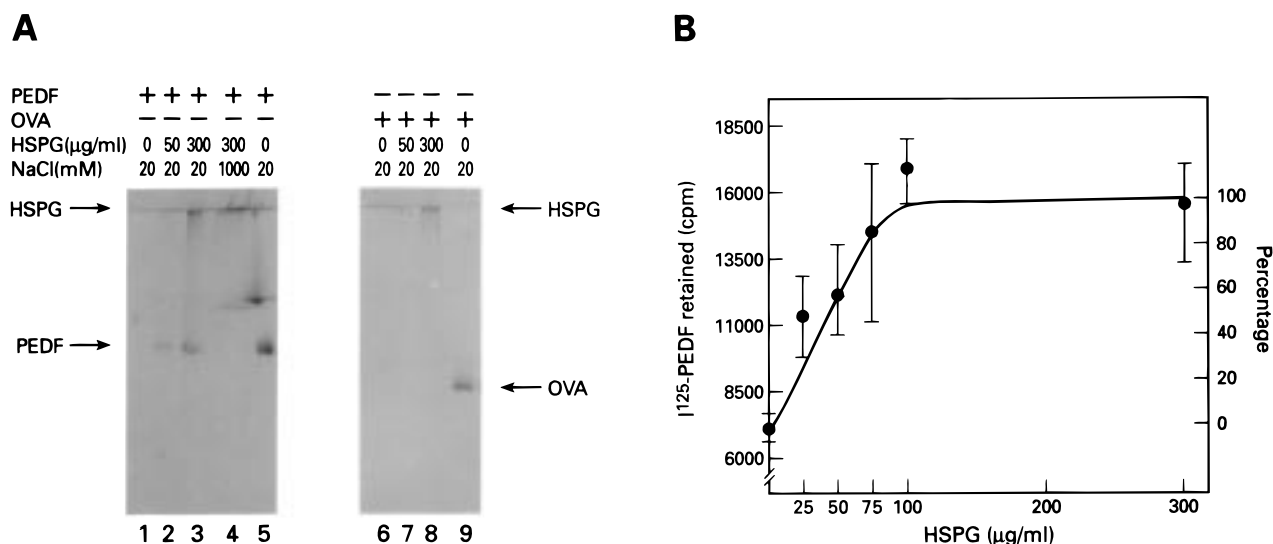


FIGURE 3: PEDF binds to heparan sulfate proteoglycan. (Panel A) PEDF–HSPG complex formation. Bovine PEDF (120  $\mu\text{g/mL}$ ) or ovalbumin (100  $\mu\text{g/mL}$ ) were mixed each with HSPG, incubated in buffer H at 4  $^{\circ}\text{C}$  for 30 min, and then subjected to ultrafiltration using membranes with a 100 000 MWCO exclusion limit to separate bound from free PEDF. The retained material was analyzed by SDS–12.5%PAGE. Photographs of Coomassie Brilliant blue stained gels are shown. PEDF and ovalbumin (OVA) and concentration of HSPG and of NaCl in the incubation buffer were added as indicated at the top of each lane. Lanes 1–4 and 6–8, retained protein from Centricon-100; lanes 5 and 9, filtered protein concentrated using Centricon-30 from lanes 1 and 6, respectively. (Panel B) Binding analysis of HSPG to PEDF. Radiolabeled [ $^{125}\text{I}$ ]PEDF (91.5 ng/mL, 6.25  $\mu\text{Ci/mL}$ ) was mixed and incubated with increasing concentrations of HSPG at 4  $^{\circ}\text{C}$  for 30 min. Binding was analyzed by ultrafiltration using Microcon-100 devices and bound radioactivity on the device quantified by liquid scintillation using a  $\beta$ -counter. To the right, retention of PEDF is given in percentage where 100% corresponds to saturation levels. PEDF binding to HSPG is in a concentration-dependent fashion with an  $\text{EC}_{50} = 40 \mu\text{g/mL}$  HSPG.

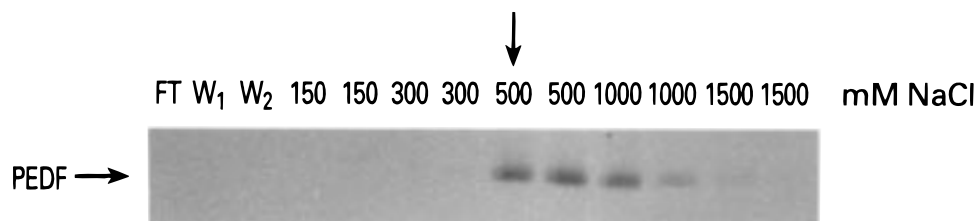


FIGURE 4: PEDF affinity for dextran sulfate. Bovine PEDF (40  $\mu\text{g}$ ) was applied to a column of sulfated dextran beads (0.5 mL) and incubated at 4  $^{\circ}\text{C}$  for 30 min in buffer H. The protein was subjected to chromatography as in Figure 2. Elution was with a step gradient of NaCl, and fractions were analyzed by SDS–PAGE followed by Coomassie blue staining. Numbers at the top of each lane correspond to NaCl concentration of each fraction. The arrow indicates the fraction at which protein starts eluting from the column.

2) was half of that with 300  $\mu\text{g/mL}$  HSPG (lane 3), the latter being 83% of the initial PEDF. PEDF retention by HSPG was not observed in the presence of 1 M NaCl (lane 4). Ovalbumin is a serpin with no known glycosaminoglycan affinity and no demonstrable inhibitory activity, and was used to define the specificity of this assay for PEDF. Figure 3A shows that ovalbumin was not retained by HSPG (lanes 6–8). To study the effects of heparin in this assay, an excess of heparin (2500  $\mu\text{g/mL}$ , <50 000 MW) was added to PEDF alone or to an HSPG/PEDF mixture. We found that, in the presence of heparin, PEDF was not retained and that the HSPG-retained fraction contained similar amounts of PEDF as the one without heparin (data not shown). These results show that PEDF retention is not due to homopolymerization induced by glycosaminoglycans and that heparin does not displace the HSPG from the HSPG–PEDF complex.

Binding analysis to HSPG was performed with radiolabeled [ $^{125}\text{I}$ ]PEDF (Figure 3B). Retention of PEDF was linear and reached saturation levels by  $\sim 100 \mu\text{g/mL}$  HSPG, and with a half-maximal specific binding  $\text{EC}_{50}$  of 40  $\mu\text{g/mL}$ . Note that the amount retained with 50  $\mu\text{g/mL}$  HSPG was half of that at saturations levels, similar to the quantitation obtained by SDS–PAGE analysis in Figure 3A. These results show

that retention of PEDF with HSPG is specific and in a concentration-dependent fashion. In addition, PEDF bound to immobilized heparan sulfate and eluted from this column with an increase in NaCl concentration (data not shown). Together, PEDF binds to HSPG in solution by forming a complex larger than 100 kDa, most likely between the protein and the heparan sulfate component of HSPG mediated by ionic interactions.

**PEDF Binds to Sulfated Dextran Column.** Dextran sulfate is a heparin-like polysaccharide composed of glucose polymers with a negative charge density higher than heparin. To determine whether PEDF has affinity for other sulfated oligosaccharides, besides glycosaminoglycans, we performed sulfated dextran column chromatography. PEDF bound to a sulfated dextran column and eluted from the column with 500 mM NaCl in buffer H (Figure 4). Thus, PEDF has a higher affinity for dextran sulfate than the glycosaminoglycans studied above.

**Biotinylation of PEDF Prevents Binding to Heparin.** Ionic interactions between protein and glycosaminoglycans are mediated by positively charged residues of the protein such as lysines, arginines, and histidines and negative charges of the glycosaminoglycan. To investigate the role for lysine

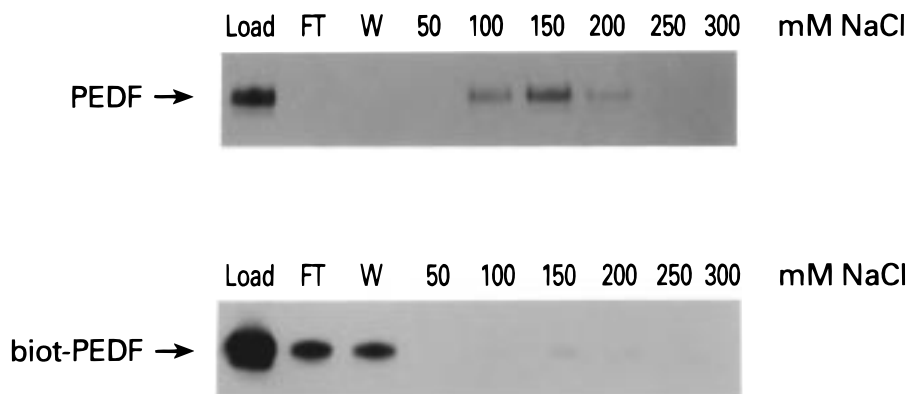


FIGURE 5: Heparin affinity column chromatography of chemically modified PEDF. Exposed lysines of recombinant human PEDF were modified by biotinylation with Sulfo-NHS-LC-biotin. The overall protein conformation of the modified protein was confirmed by limited proteolysis (data not shown). Unmodified PEDF and biotinylated PEDF (4.2 mol of biotin/mol of PEDF) were subjected to heparin affinity column chromatography. Fractions from the elution with a NaCl step-gradient were analyzed by SDS–10 to 20% gradient PAGE. For unmodified PEDF, the gel was stained with Coomassie Brilliant blue. Detection of biotinylated PEDF was performed after western transfer to nitrocellulose by chemiluminescence of an avidin–horseradish peroxidase complex. Biotinylated PEDF loses its heparin binding affinity.

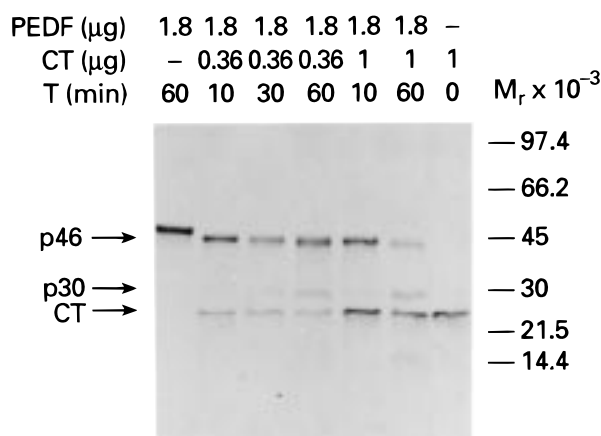


FIGURE 6: Controlled proteolysis of PEDF with  $\alpha$ -chymotrypsin. PEDF was mixed with  $\alpha$ -chymotrypsin in 20 mM Tris HCl, pH 7.5, 150 mM NaCl, and 1 mM EDTA and incubated at 25 °C for the indicated time. Reactions were stopped by freezing in dry ice and the addition of SDS–PAGE sample buffer. Mixtures were analyzed by SDS–10 to 20% gradient PAGE under nonreducing conditions. Photograph of a Coomassie Brilliant blue stained gel is shown. The arrows on the left denote the positions of the limited products of the reaction (p46 and p30) and  $\alpha$ -chymotrypsin (CT).

residues of PEDF in heparin binding, recombinant human PEDF protein (rhPEDF) was chemically modified by biotinylation using an activated *N*-hydroxysuccinimide ester form of biotin that reacts with primary amines such as those in lysines. Limited proteolysis analysis of chemically modified and unmodified proteins showed that both shared an overall protein conformation (data not shown). Figure 5 shows that unmodified rhPEDF bound to heparin and eluted with 100–200 mM NaCl with a peak at 150 mM NaCl, while the biotinylated protein did not bind to the heparin column. This result shows that lysine residues of the protein are involved in the interactions between PEDF and heparin.

**Heparin Affinity of PEDF Polypeptide Fragments.** To localize the region involved in heparin binding, we prepared polypeptide fragments by controlled proteolysis of bovine PEDF. As with other serpins, PEDF has a protease-sensitive region at its serpin-exposed loop, and specifically, it has a chymotryptic cleavage site between the P1 and P1' positions (27, 19). A 46 kDa PEDF polypeptide fragment, p46, was prepared by controlled proteolysis with a chymotrypsin:

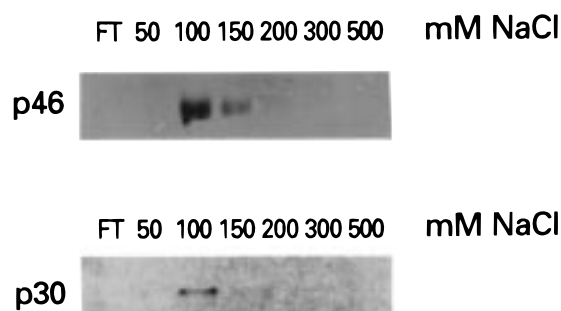


FIGURE 7: Heparin affinity column chromatography of PEDF polypeptide fragments. PEDF polypeptide fragments were prepared by controlled proteolysis with  $\alpha$ -chymotrypsin. Fragment p46 was obtained at a protease:substrate ratio of 1:100 (w/w) and p30 at a ratio of 1:1 (w/w). The reaction mixtures were analyzed by heparin affinity column chromatography. Fractions from the column were resolved by SDS–10 to 20% gradient PAGE. Photographs of a Coomassie Brilliant blue stained gel is shown for p46 and of an immunoblot using Ab-rPEDF for p30. PEDF fragments p46 and p30 have binding affinity for heparin.

PEDF ratio of 1:100 (w/w) and contained residues between positions 21–382. Treatments with a higher chymotrypsin: PEDF ratio (20:100 and 56:100) generated a less abundant fragment of 30 kDa (p30), in addition to the p46 fragment (Figure 6). Yields of the p30 polypeptide augmented with incubation time and with a higher protease:substrate ratio; however, these p30 products were more labile to further degradation upon storage. Products of 20 kDa or less were not detected, suggesting that these had been completely proteolyzed. A limited proteolytic product of 30 kDa was not observed with trypsin treatments. Sequence analysis of p30 polypeptide revealed that its amino-terminal region was identical to that of p46 and the intact protein. From its migration in SDS–PAGE, we estimated that the p30 fragment maps to residue positions 21–~260. Reaction mixtures containing the p46 and p30 were used for analysis (Figure 7). The results show that the p46 and p30 polypeptides had similar affinities for heparin (100 mM NaCl). Their affinities were slightly lower than that of the intact protein (peak at 150 mM NaCl). Thus, PEDF without its serpin-exposed loop retains the apparent affinity for heparin, and even when larger truncations from the C-terminal end of PEDF are removed, the affinity for heparin is retained.

			-----helix D-----	
ATIII	114	<b>K</b>	- T S D Q I H F F F A <b>K</b> L N C <b>R</b> L Y <b>R</b> <b>K</b> A	134
PN1	63	<b>R</b>	Y N V N G V G <b>K</b> I L <b>K</b> <b>K</b> I N <b>K</b> A I V S <b>K</b> <b>K</b>	84
HCII	173	<b>K</b>	Y E I T T I H N L F <b>R</b> <b>K</b> L T H <b>R</b> L F <b>R</b> <b>R</b> N	194
PAI	65	<b>K</b>	I D D <b>K</b> G M A P A L <b>R</b> H L Y <b>K</b> E L M G P W	105
hPEDF	112	L	I S S P D I H G T Y <b>K</b> E L L D T V T A P Q	133
bPEDF	110	L	I I N P D I H G T Y <b>K</b> D L L A S V T A P Q	131
OVA	74	C	G T S V N V H S S L <b>R</b> D I L N Q I T <b>K</b> P N	96

FIGURE 8: Sequence comparison of proposed heparin-binding regions of PEDF and other serpins. Selected sequences of antithrombin III (ATIII), protease nexin-1 (PN-1), heparin cofactor II (HCII), plasminogen activator inhibitor-1 (PAI-1), and ovalbumin, a nonheparin-binding serpin, are aligned with human PEDF (hPEDF, accession number M76979), bovine PEDF (bPEDF, accession number U482229), and ovalbumin (OVA). Secondary structure is given at the top and aligned as described by Huber and Carrell (43). Lysine and arginine residues are in bold. Note that PEDF does not share homology in basic residues at helix D, the primary heparin binding site of antithrombin III, with the last three of the five residues changed to uncharged and one reversed to an acidic residue.

**Molecular Modeling of PEDF.** Alignment and comparison of sequences of PEDF and heparin-binding serpins indicated that PEDF does not share homology in helix D, the primary heparin-binding site of antithrombin III (Figure 8). Since unfolding of PEDF eliminated its binding affinity for glycosaminoglycans, determinants for this interaction may be identified in its tertiary conformation. We have used computer-assisted molecular modeling to identify the putative glycosaminoglycan-binding region of PEDF, in particular, to identify clusters of basic residues on the protein surface that could be involved in the electrostatic binding of glycosaminoglycans/polyanions. The averaged surface electrostatic potential from two models, PEDF<sub>OVA</sub> and PEDF<sub>ATIII</sub> constructed based on the structures of ovalbumin (a noninhibitory, nonheparin-binding serpin) and antithrombin III (an inhibitory, heparin-binding serpin), respectively, was calculated and analyzed (Figure 9). Examining helix D, we found that PEDF lacks a basic cluster surface potential but has a negative charge. However, the surface potential of PEDF revealed a cluster of exposed basic residues on an area located on the large central  $\beta$ -sheet A that extends from the C-terminus of helix F to the end of the sheet in a direction diametrically opposite to the homologous serpin reactive site P1 (Figure 9A). The area is composed of residues (K134, K137, K189, K191, H212, and K214) that define a "cleft" that expands to more convex regions with basic residues (R141, R165, R167, K146, K147, and R149). The basic cleft region of PEDF provides the main positive charge available to interact with glycosaminoglycans/polyanions with a location that differs from previously described heparin-binding sites for serpins. Interestingly, rotation of the molecule about 180° with respect to this basic region revealed an extensive negative potential on its opposite side (Figure 9B).

## DISCUSSION

Here, we have shown that PEDF binds to glycosaminoglycan/polyanion macromolecules with interactions primarily ionic in nature. A putative glycosaminoglycan-binding site can be identified on PEDF. Although proteins and glycosaminoglycans form extracellular matrixes, glycosaminoglycans confer the main negative charge to these complex matrixes. In particular, we have shown binding to those types of glycosaminoglycans known to coexist with PEDF in the interphotoreceptor matrix, e.g., chondroitin, heparan sulfates. The fact that the efficiencies of PEDF extractions

from the interphotoreceptor matrix and PEDF elutions from immobilized glycosaminoglycans with increasing NaCl concentrations (0.02–0.5 M) are similar suggests an association of PEDF with glycosaminoglycan components of the interphotoreceptor matrix. The observed increase in PEDF extraction with even higher NaCl concentrations (1.5 M) suggests an association with other polyanions by higher ionic strength. Therefore, the glycosaminoglycan/polyanion-binding property of PEDF represents the likely molecular basis for its association with extracellular matrixes.

Comparison among serpin members reveals that, although PEDF is similar to ovalbumin in the lack of demonstrable serine protease inhibitory activity and the serpin conformational change upon cleavage at the serpin exposed loop (27), it differs from ovalbumin in glycosaminoglycan binding (Figures 2 and 3). We found that the apparent binding affinities of native PEDF for glycosaminoglycans are modest. Interestingly, these are in the same range as those of heparin cofactor II for heparin and chondroitin sulfate B (0.12–0.16 M NaCl) (ref 34, Figure 2), but lower than the heparin affinity of protease nexin-1 and antithrombin III (0.6–0.7 M NaCl) (35, 36). Van Nostrand et al. (35) have characterized a low abundant form of protease nexin-1 that is indistinguishable from the most abundant form in structural characteristics and in heparin-dependent inhibitory activity against thrombin, but has lower heparin- and dextran sulfate-binding affinities (0.3 M NaCl and 0.6 M NaCl, respectively) that are more comparable to PEDF. Although the length of heparan sulfate chains in the HSPG used in this study is undefined, comparison of the half-maximal specific binding of native bovine protein (~40  $\mu$ g/mL HSPG) and the  $K_d$  of rhuPEDF with heparin of a defined length  $M_r \sim 9000$  ( $K_d = 4.1 \pm 0.3 \mu$ M or 37  $\mu$ g/mL) (23) reveal similar binding affinities for heparin and HS of both proteins. Binding to glycosaminoglycans is not known for other noninhibitory serpins, such as angiotensinogen and maspin.

The negatively charged nature of glycosaminoglycans immediately suggests that its binding to proteins may be achieved by electrostatic interactions with basic residues in a binding site on the surface of the protein. This has been confirmed in several studies that attempt to identify critical residues of a protein involved in heparin binding (see ref 37). The involvement of positively charged residues of PEDF in the heparin binding was analyzed following chemical modification of primary amines of positively



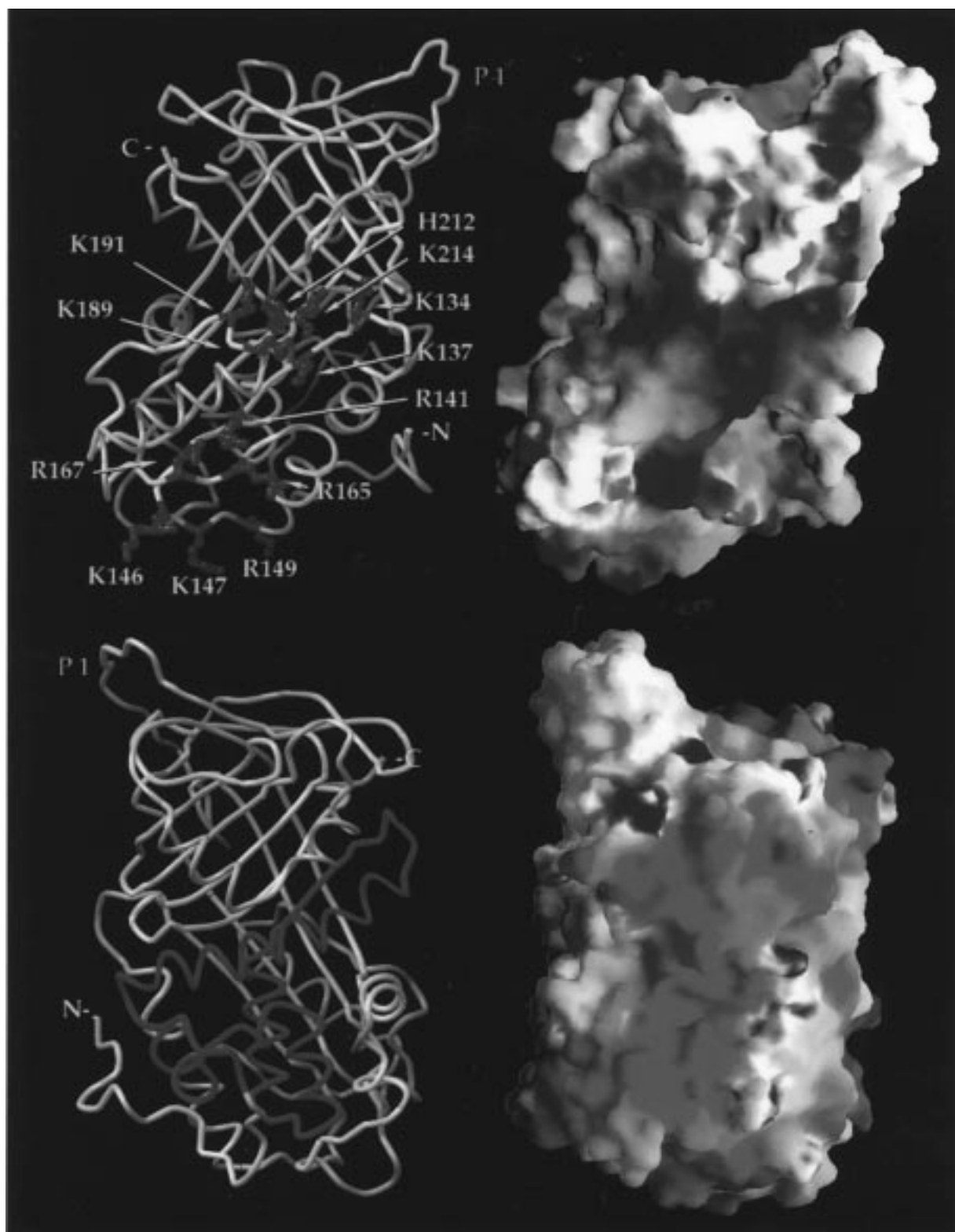


FIGURE 9: Illustration of the proposed basic, heparin-binding areas and acidic areas mapped to the homology model of PEDF. (Above, left) Backbone tracing (gray) of the PEDF model with the clusters of basic residue side chains shown in ball-and-stick representations (blue). Only the PEDF model based on antithrombin III is shown. (Right) electrostatic surface potential (averaged from the two PEDF models, on ovalbumin and antithrombin III) shown from the same orientation. Negative potentials are shown in red, positive potentials in blue and neutral in white. This side has essentially a basic potential. Note a basic cleft at the center of the molecule. (Below) Opposite side view of the model shown in the above panels. (Left) Oriented to this side is a region spanning between human PEDF positions 44–121, previously shown to contain the neurotrophic active site (2), shown in green. (Right) This side has a negative electrostatic potential. Other features of the model are labeled: “N” and “C” for amino- and carboxy-termini and “P1” for the homologous serpin reactive site.

charged lysine residues (Figure 5). The molar incorporation ratio of about 4:1 biotin/PEDF implies that only a subset of the 22 lysine residues of the molecule need to be modified

to affect heparin binding. The effects of chemical modification on heparin binding are due primarily to the loss of the positive charge on the exposed lysine residues. However,



we cannot rule out the possibility that the effects on binding result from steric blocking by biotin groups or by alteration of the tertiary structure of the glycosaminoglycan-binding domain in PEDF.

The fact that PEDF loses its heparin-binding affinity when in urea indicates that protein unfolding affects its ability to interact with heparin or that there is interference with hydrogen bonding (Figure 2). The heparin-binding region of PEDF was analyzed following limited proteolysis, which is known to yield polypeptide fragments with folded conformation similar to that of the native protein. Incubation of PEDF with several proteases proves that the homologous serpin-reactive region is in a conformation that is accessible to proteolytic cleavage (27). Uncleaved and cleaved-PEDF (p46) have similar stability toward thermal and guanidinium hydrochloride denaturation (27, 23), suggesting that the tertiary structure in the intact protein and p46 is also similar. Treatments with chymotrypsin yield an N-terminal polypeptide fragment, p30, less resistant to degradation than p46, and similar to chymotrypsin-treated ovalbumin [Figure 6 (37)]. This reveals a second protease sensitive region (around PEDF position 260) in these two serpins. PEDF does not lose its heparin-binding affinity upon cleavage at its serpin-exposed loop (Figure 7), similar to protease nexin-I but unlike antithrombin III (36). The heparin-binding region is maintained even when further cleavage from the carboxy-end of PEDF is accomplished, indicating that the region from 21 to ~260 is sufficiently stable to maintain the tertiary structure of the heparin-binding region.

In contrast to other heparin-binding serpins, PEDF does not share homology with antithrombin III in basic residues at the predicted helix D, its primary heparin-binding site (Figure 8). In addition, the surface potential of PEDF shows a cluster of negative charge at the surface of helix D. However, inspection of the PEDF model reveals a positively charged region in another location of the molecule that is densely populated with exposed lysine residues that are available to interact with glycosaminoglycans and other polyanions (Figure 9A). We believe that the negatively charged glycosaminoglycans bind by anchoring onto the positively charged cleft region at the center of  $\beta$ -sheet A—strands 2 and 3—and helix F (K134, K137, K189, K191, H212, and K214), and this is the putative glycosaminoglycan/polyanion-binding site for PEDF. The dispersed positions in the linear sequence of these basic residues explain the need for a folded protein conformation to maintain the heparin binding property. To support our observations, addition of an excess of heparin to PEDF results in an enhancement of fluorescence due to the surface-exposed tryptophan 183, which is in helix F in the same side and near the heparin-binding cleft (23). Interestingly, position H212 in the human PEDF is changed to Y210 in the bovine sequence, possibly explaining the slightly higher affinity of the human protein (Figures 2 and 5). Homologous regions in antithrombin III and ovalbumin three-dimensional structures do not display a positive surface potential as in PEDF. Thus, this basic cleft identified in PEDF is different from the ones described for other serpins. Further structure—function studies using mutagenesis will confirm the relevance of this location in glycosaminoglycan binding of PEDF.

The spatial relationship of the PEDF glycosaminoglycan-binding area and neurotrophic-active region results in

interesting observations. The region spanning 44–121, which we have previously shown to contain the neurotrophic active region (27), is oriented toward the side opposite the glycosaminoglycan-binding site, the side that has a negative surface potential. Both sites are distant from the serpin-exposed loop, consistent with the heparin-binding affinity and neurotrophic activity of p46. Thus, these two regions, the glycosaminoglycan-binding region and the neurotrophic active site, are two distinct and nonoverlapping areas of the PEDF protein.

In summary, PEDF represents a class of glycosaminoglycan-binding serpins with a binding site predicted to be in a novel location for members of the serpin family. This property of PEDF forms the molecular basis for its association with extracellular matrixes. We have shown before that a small polypeptide fragment of PEDF containing a neurotrophic active site is sufficient for neurotrophic activity (27). However, it is not known yet whether the properly folded native protein requires cell-surface-associated glycosaminoglycans for the interaction of its neurotrophic region with cell surface receptors, as shown for other factors. Further studies are needed to determine what direct effects these polysaccharides have on the biochemical interactions between PEDF and receptors on neuronal cells. In addition to binding in vitro, the interactions of PEDF and glycosaminoglycans may serve to localize PEDF activity in the CNS.

## ACKNOWLEDGMENT

We thank Dr. Barbara Wiggert for use of densitometric scanner and proof reading this manuscript, Dr. Mark Wardell for providing coordinates for antithrombin III prior to release under the PDB designation 2ANT, Ms. Patricia Spinella for protein sequencing determination, Miss Emily Cartwright for assistance in chromatography and SDS—PAGE, and Dr. Timothy Mueser for helpful suggestions and for comments on the manuscript.

## REFERENCES

- Schlessinger, J., Lax, I., and Lemmon, M. (1995) *Cell* 83, 357–360.
- Hassell, J. R., Kimura, J. H., and Hascall, V. C. (1986) *Annu. Rev. Biochem.* 55, 539–567.
- Brittis, P. A., Canning D. R., and Silver, J. (1992) *Science* 255, 733–736.
- Hageman, G. S., and Johnson, L. V. Structure and function of the retinal interphotoreceptor matrix. *Progress in Retinal Research*, Vol. 10, pp 207–245, Pergamon Press, New York.
- Adler, A. J., and Klucznick, K. M. (1982) *Exp. Eye. Res.* 43, 23–434.
- Morris, J. E., Hopwood, J. J., and Dorfman, A. (1977) *Dev. Biol.* 58, 313–327.
- Chai, L., and Morrin, J. E. (1994) *Curr. Eye Res.* 13, 669–677.
- Karthikayan, L., Flad, M., Engel, M., Myer-Puttlitz, B., Margolis, R. W., and Margolis, R. K. (1994) *J. Cell. Sci.* 107, 3213–3222.
- Landers, R. A., Rayborn, M. E., Myers, K. M., and Hollyfield, J. G. (1994) *J. Neurochem.* 63, 737–7501.
- Bollineni, J. S., Alluru, I., and Reddi, A. S. (1997) *Curr. Eye Res.* 16, 127–130.
- Kliffen, M., Mooy, C. M., Luiders, T. M., Huijman, J. G., Kerkvliet, S., and de Jong, P. T. (1996) *Arch. Ophthalmol.* 114, 1009–1014.
- Burgess, W. H., and Maciag, T. (1989) *Annu. Rev. Biochem.* 58, 575–606.

13. Brickman, Y. G., Ford, M. D., Small, D. H., Bartlett, P. F., and Nurcombe, V. (1995) *J. Biol. Chem.* 270, 24941–24948.
14. Gitay-Goren, H., Soker, S., Vlodavsky, J., and Neufeld, G. (1992) *J. Biol. Chem.* 267, 6093–6098.
15. Farrell, G. H., and Cunningham, D. D. (1987) *Biochem. J.* 245, 543–550.
16. Walz, A., McFarlane, S., Brickman, Y. G., Nurcombe, V., Bartlett, P. F., and Holt, C. E. (1997) *Development* 124, 2421–2430.
17. Burg, M. A., Halfter, W., and Cole, G. J. (1995) *J. Neurosci. Res.* 41, 49–64.
18. Wu, Y.-Q., Notario, V., Chader, G. J. and Becerra, S. P. (1995) *Protein Expression Purif.* 6, 447–456.
19. Wu, Y.-Q., and Becerra, S. P. (1996) *Invest. Ophthalmol. Visual Sci.* 37, 1984–1993.
20. Ortego, E., Escribano, J., Becerra, S. P., and Coca-Prados, M. (1996) *Invest. Ophthalmol. Visual Sci.* 37, 2759–2767.
21. Steele, F. R., Chader, G. J., Johnson, L. V., and Tombran-Tink, J. (1993) *Proc. Natl. Acad. Sci. U.S.A.* 90, 1526–1530.
22. Pignolo, R. J., Cristofalo, V. J., and Rotenberg, M. O. (1993) *J. Biol. Chem.* 268, 8949–8957.
23. Stratikos, E., Alberdi, E., Gettins P. G. W., and Becerra, S. P. (1996) *Protein Sci.* 5, 2575–2582.
24. Tombran-Tink, J., Chader, G. J., and Johnson, L. V. (1991) *Exp. Eye Res.* 53, 411–414.
25. Taniwaki, T., Becerra, S. P., Chader, G. J., and Schwartz, J. P. (1995) *J. Neurochem.* 64, 2509–2517.
26. Taniwaki, T., Hirashima, N., Becerra, S. P., Chader, G. J., Etcheberrigaray, R., and Schwartz, J. P. (1997) *J. Neurochem.* 68, 26–32.
27. Becerra, S. P., Sagasti, A., Spinella, P., and Notario, V. (1995) *J. Biol. Chem.* 270, 25992–25999.
28. Green, N. M. (1975) *Adv. Protein Chem.* 29, 85–133.
29. Stein, P. E., Leslie, A. G., Finch, J. T., and Carrell, R. W. (1991) *J. Mol. Biol.* 221, 941–959.
30. Skinner, R., Abrahams, J. P., Whisstock, J. C., Lesk, A. M., Carrell, R. W., and Wardell, M. R. (1977) *J. Mol. Biol.* 266, 601–609.
31. Abola, E. E., Bernstein, F. C., Bryant, S. H., Koetzle, T. F., and Weng, J. (1987) Protein Data Bank. in *Crystallographic Databases-Information Content, Software Systems, Scientific Applications* (Allen, F. H., Bergerhoff, G., and Sievers, R. Eds.) pp 107–132, Data Commission of the International Union of Crystallography, Bonn/Cambridge/Chester.
32. Bernstein, F. C., Koetzle, T. F., Williams, G. J. B., Meyer, Jr., E. F., Brice, M. D., Rodgers, J. R., Kennard, O., Shimanouchi, T., and Tasumi, M. (1977) *J. Mol. Biol.* 112, 535–542.
33. Bairoch, A., and Apweiler, R. (1996) *Nucleic Acids Res.* 24, 21–25.
34. Tollefsen, D. M., Majerus, D. W., and Blank, M. K. (1982) *J. Biol. Chem.* 257, 2162–2169.
35. Van Nostrand, W. E., Wagner, S. L., and Cunningham, D. D. (1988) *Biochemistry* 27, 2176–2181.
36. Evans, D. L., McGrogan, M., Scott, R. W., and Carrell, R. W. (1991) *J. Biol. Chem.* 266, 22307–22312.
37. Margalit, H., Fischer, N., and Ben-Sasson, S. A. (1993) *J. Biol. Chem.* 268, 19228–19231.

BI9802317